analytical chemistry

Article

pubs.acs.org/ac

Direct Detection of DNA below ppb Level Based on Thionin-Functionalized Layered MoS_2 Electrochemical Sensors

Tanyuan Wang, Ruizhi Zhu, Junqiao Zhuo, Zhiwei Zhu, Yuanhua Shao, and Meixian Li*

Institute of Analytical Chemistry, College of Chemistry and Molecular Engineering, Peking University, Beijing 100871, P.R. China

Supporting Information

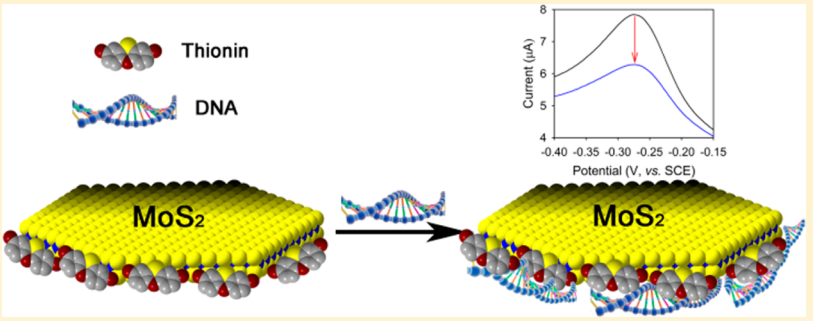

ABSTRACT: A layered MoS_2–thionin composite was prepared by sonicating their mixture in an ionic liquid and gradient centrifugation. Because DNA is rarely present in single-stranded form, either naturally or after PCR amplification, the composite was used for fabrication of a double-stranded DNA (dsDNA) electrochemical biosensor due to stable electrochemical response, intercalation, and electrostatic interaction of thionin with DNA. The linear range over dsDNA concentration from 0.09 ng mL^{-1} to 1.9 ng mL^{-1} is obtained, and moreover, it is suitable for the detection of single-stranded DNA (ssDNA). The biosensor has been applied to the detection of circulating DNA from healthy human serum, and satisfactory results have been obtained. The constructed DNA electrochemical biosensor shows potential application in the fields of bioanalysis and clinic diagnosis. Furthermore, this work proposes a new method to construct electrochemical biosensors based on MoS_2 sheets.

The sensitive and selective detection of DNA has become a subject of intense research during recent years due to its potential application in the fields of pharmacogenetics, pathology, genetics, and food safety,[1−4] and various DNA sensors have been reported.[5,6] Among them, electrochemical DNA sensors attract much more attention on account of their high sensitivity and selectivity, portability, rapid response, and low cost.[7−9] Especially, nanomaterials such as carbon nanotubes,[10,11] graphene,[12,13] and gold nanoparticles[14,15] have been used to construct electrochemical DNA sensors to achieve extremely sensitive detection of DNA owing to their good electronic properties and large specific surface areas. But so far most of the reported DNA sensors have been applied to the detection of selected DNA sequences.[16,17] Few studies on the electrochemical detection of double-stranded DNA (dsDNA) are reported. In fact, DNA is rarely present in single-stranded form, either naturally or after PCR amplification. Improvements in the detection of dsDNA or natural DNA should lead to more robust and flexible DNA diagnostics.[18] For example, the concentration of circulating DNA in human plasma/serum is suggested to be an indicator for a variety of tumors,[19,20] and the concentration of circulating DNA in a healthy person's serum is usually much lower than that in a cancer patient's serum. Therefore, the construction of a natural DNA sensor has become a practical research topic.

As a kind of layered material, MoS_2 attracts great attention in the fields of nanoelectronics and optoelectronics.[21,22] Moreover, its catalytic performance toward hydrogen evolution reaction (HER)[23,24] and oxygen reduction reaction (ORR)[25,26] makes it a promising material in the fields of energy conversion and storage. Besides, its unique electronic and electrochemical properties, large specific surface area, and potential for surface modification imply that it could also be applied in the field of biosensing. However, until now just little research has been done in this aspect.[27−29] On the other hand, thionin is a kind of cationic phenothiazine dye that can show electrochemical activity.[30,31] It can bind strongly to dsDNA through intercalation and electrostatic interaction to lead to a decrease in its own redox signal when modified on the electrode.[32] What is more, it can be attached on the surface of carbon nanotubes or $Mo_6S_{9-x}I_x$ nanowires,[32,33] which insinuates that it may also be used to modify MoS_2 nanosheets and constructed DNA biosensors. Herein, we prepared a layered MoS_2-thionin composite by an extremely easy combination method of ultrasonication and gradient centrifugation to construct a sensitive DNA electrochemical sensor. The DNA sensor could even work with the

Received: July 25, 2014
Accepted: November 13, 2014

   dx.doi.org/10.1021/ac5027786 | *Anal. Chem.* XXXX, XXX, XXX–XXX

existence of relatively high concentration of protein, and it could detect the concentration of circulating DNA in human serum.

EXPERIMENTAL SECTION

Preparation of MoS_2–Thionin Composite. Thionin acetate salt (for microscopy, Aldrich) was dissolved in 1-butyl-3-methylimidazolium hexafluorophosphate (97.0%, Aldrich) with a concentration of 10 mg mL^{-1}. Then MoS_2 (99%, 2 μm in size, Aldrich) was added to the mixture with a concentration of 10 mg mL^{-1}. This mixture was ultrasonicated by a SB-2200 sonifier (Shanghai Branson, China) at room temperature (22 ± 2 °C) for 2 h. After that the suspension was centrifuged at 2000 rpm for 20 min to remove the large particles. The supernatant was collected and centrifuged at 6000 rpm for 20 min to obtain precipitation. Then the precipitation was gathered and washed with DMF (99.9%, Aldrich) to remove the free thionin until the supernatant was colorless. For a comparison, the bulk MoS_2 was also ultrasonicated and centrifuged in 1-butyl-3-methylimidazolium hexafluorophosphate in the absence of thionin to obtain the MoS_2 sheets. The MoS_2/thionin mixture was fabricated by simply mixing MoS_2 sheets with thionin acetate salt in DMF. A GS-15R centrifugation system (Beckman, America) was used for these procedures.

Fabrication of DNA Biosensors Based on MoS_2–Thionin Composite. MoS_2-thionin composite was dispersed into DMF with a concentration of approximately 2 mg mL^{-1}. Then the solution was dropped on the glassy carbon (GC) electrodes (Φ = 3 mm) and dried in the air with a loading of 0.1 mg cm^{-2}. This modified electrode was then washed with deionized water for five times to avoid the possible influence of the residual DMF on the following experiments. The MoS_2 sheets and MoS_2/thionin mixture (the exfoliated MoS_2 sheets were mixed with thionin directly in DMF) were also modified on the GC electrodes with the same procedure for comparison.

Characterization. All electrochemical measurements were carried out on a CHI 660D (Chenhua, China) at room temperature. A Pt electrode was used as the counter electrode and a modified electrode was used as the working electrode. A saturated calomel electrode (SCE) was used as the reference electrode for all the electrochemical tests. All the solutions were saturated with N_2 during the cyclic voltammetric (CV) and square wave voltammetric (SWV) measurements. For SWV measurements, the incremental potential was set to be 4 mV with a frequency of 15 Hz and the amplitude was 25 mV. Deoxyribonucleic acid (dsDNA) sodium salt from salmon sperm with molecular weight of 50 000–100 000 Da was bought from ACROS Organics (CAS: 68938-01-2). Its ratio of UV absorbance at 260 and 280 nm in 0.18 M NaCl was calculated to be 1.8, which indicated that the DNA sample was sufficiently free of protein and RNA. The concentration of the standard DNA stock solution was spectrophotometrically determined to be 0.940 mg mL^{-1} by measuring the absorbance of the diluted solution at 260 nm. The dsDNA was denatured by heating at 100 °C for 10 min in a mixed solution of 15 mM NaCl and 1.5 mM sodium citrate and quick cooling in an ice bath.[34] The denatured DNA was then tested for a comparison. Single-stranded DNA (ssDNA) from calf thymus (Aldrich) and ribonucleic acid (RNA) from torula yeast (Aldrich) were also used for the measurements. The human circulating DNA was extracted from human serum by using a circulating nucleic acid kit (CWbiotech, China). Briefly, protease was used to degrade the protein in the serum. Then the ionic strength of the solution was enhanced and an adsorption column was used to extract DNA from the mixture. After that the column was washed with buffer and DNA was then eluted from the column by water. 3.5 mL of human serum was used for the extraction process each time and the extracts were added to the N_2 saturated 0.1 M PBS for measurements. A transmission electron microscopy (TEM) image was acquired on a JEM-2100F electron microscope (JEOL, Japan). Scanning electron microscopy (SEM) images were obtained on an S-4800 electron microscope (Hitach, Japan). X-ray photoelectron spectra (XPS) were collected on an Axis Ultra spectrometer (Kratos Analytical Ltd., Japan) and the binding energy was calibrated by the C 1s peak at 284.8 eV. UV–vis absorption spectra were recorded on a U-4100 UV–vis-NIR spectrophotometer (Hitach, Japan).

RESULTS AND DISCUSSION

The layered MoS_2–thionin composite was fabricated with the assistance of ionic liquid by a one-step ultrasonication method. Earlier works have proved that ultrasonication is an effective way to exfoliate MoS_2 into nanosheets or even nanoparticles.[35−37] In this work, MoS_2 sheets were exfoliated from bulk MoS_2 by using 1-butyl-3-methylimidazolium hexafluorophosphate as the solvent and thionin was modified on the MoS_2 sheets during the exfoliation process. Figure 1 is the TEM and SEM images of the

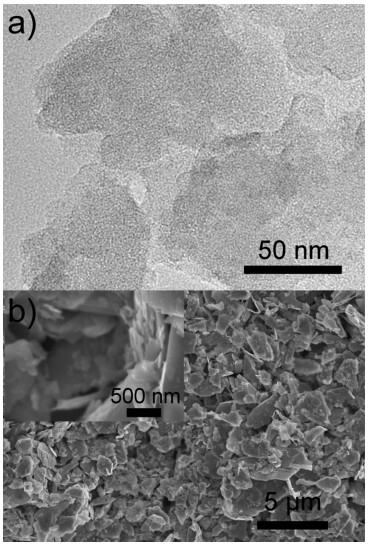

Figure 1. (a) TEM image of the MoS_2–thionin composite. (b) SEM image of the MoS_2–thionin composite.

composite. Layered structures with sizes of hundreds of nanometers could be observed. This result is similar to the MoS_2 sheets obtained by exfoliating in the organic solvent,[35] thus indicating that MoS_2 exists mainly in the form of MoS_2 sheets in the MoS_2-thionin composite, which is different from the raw bulk MoS_2. The MoS_2 sheets exfoliated by this method also demonstrate similar structure to the MoS_2-thionin composite (Figures S-1 ∼ S-2). The main reason is that thionin molecules are very small. They could not be observed by TEM and SEM characterizations.

XPS was then used to characterize the elemental composition and bonding configuration of the composite as well as the MoS_2 sheets because there was no obvious difference in morphology between them. Figures S-3 ∼ S-6 are the XPS survey spectra of the MoS_2 sheets, thionin, MoS_2–thionin composite, and MoS_2/thionin mixture, while Figure 2 is the spectra of the S 2p region for the four kinds of materials. An obvious change in S 2p binding

dx.doi.org/10.1021/ac5027786 | Anal. Chem. XXXX, XXX, XXX–XXX

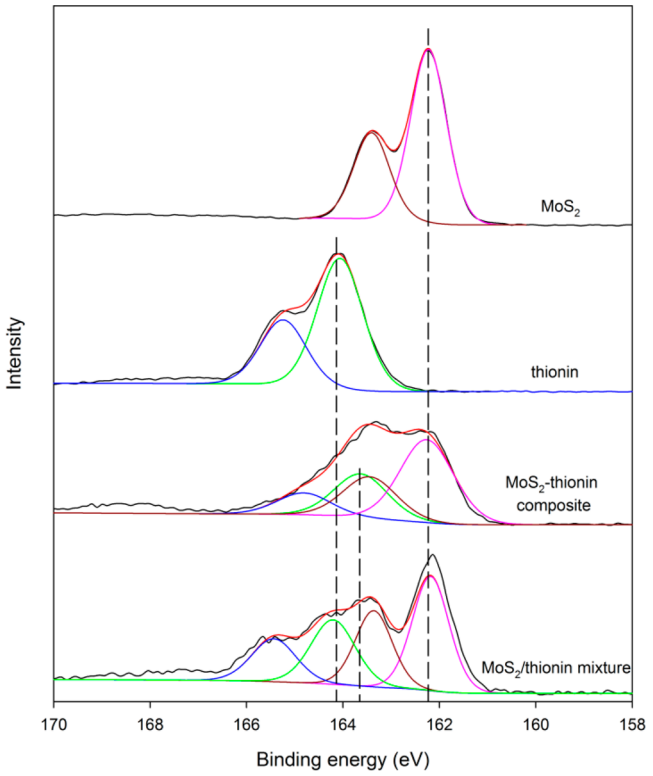

Figure 2. XPS spectra of S 2p region for the MoS_2 sheets, thionin, MoS_2−thionin composite, and MoS_2/thionin mixture, respectively.

energy could be observed for the composite. The MoS_2 sheets show a pair of S 2p peaks with the S $2p_{3/2}$ binding energy at 162.3 eV. Thionin also exhibits a couple of S 2p peaks with the S $2p_{3/2}$ binding energy of 164.1 eV. The MoS_2−thionin composite demonstrates two pairs of S 2p peaks. One with the binding energy of 162.3 eV matches well with the S $2p_{3/2}$ peak of the MoS_2 sheets. However, the binding energy of another S $2p_{3/2}$ peak for the composite is only 163.6 eV, which is lower than the S $2p_{3/2}$ binding energy of thionin. On the other hand, the S $2p_{3/2}$ binding energies of the MoS_2/thionin mixture are nearly the same as sole MoS_2 and thionin. These phenomena suggest that there is interaction between MoS_2 sheets and thionin in the composite. Thionin may accept electrons from the MoS_2 sheets and lead to this decrease in binding energy. The reason for no obvious shift in binding energy for MoS_2 sheets in the composite is that the chemical environment of the planar S atoms in the sheets has almost no change during the modification process. Hence the most possible binding site for thionin is the S edge of the MoS_2 sheets which only occupies a small portion. The report that the S edge of MoS_2 could be modified by using thiol chemistry[38] helps to prove this surmise. What is more, thionin is positively charged, which means that it could be more easily attached on the negatively charged S edge of MoS_2.[32] Therefore, thionin may bind to the S edge of the MoS_2 nanosheets. The S $2p_{3/2}$ peak with lower binding energy of the composite is in the same place with the S $2p_{3/2}$ peak of the MoS_2 sheets due to the inert nature of the planar S, while the S $2p_{3/2}$ peak with higher binding energy of the composite shifts due to the interaction between thionin and MoS_2 edges.

UV−vis absorption spectroscopy was further used to characterize the interaction between MoS_2 sheets and thionin. Figure 3 shows the absorption spectra of MoS_2 sheets, thionin, MoS_2−thionin composite, and MoS_2/thionin mixture with DMF

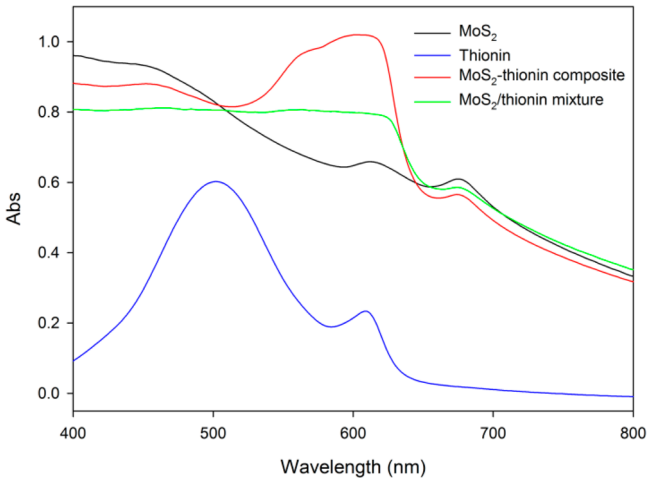

Figure 3. UV−vis spectra of MoS_2 sheets, thionin, MoS_2−thionin composite, and MoS_2/thionin mixture in DMF.

as the solvent. Thionin displays two obvious absorption peaks at about 500 and 610 nm separately, while MoS_2 exhibits several weak peaks at 450, 610, and 675 nm. The MoS_2−thionin composite also shows two weak peaks at 450 and 675 nm that corresponding to the absorption spectra of MoS_2. But in addition to these two peaks, it demonstrates another two broad peaks at 560 and 618 nm, which are mainly ascribed to the red shifts of absorption peaks of thionin in the MoS_2−thionin composite due to the synergistic charge-transfer between thionin and MoS_2 sheets. The result matches well with the XPS result. The MoS_2/thionin mixture only displays a broad and intense absorption band, and the typical absorption peaks of thionin could not be observed, which is different from that of the composite. The possible reason for this is that the strong scattering of the MoS_2 sheets causes fake absorption. Therefore, both XPS and UV−vis characterizations prove that the long-time sonication of MoS_2 and thionin mixture results in interaction between MoS_2 sheets and thionin.

In order to verify the presence and immobilization of thionin on the composite, the composite was modified on a GC electrode, and its electrochemical property was studied in 0.1 M PBS (pH = 7.4) with the protection of N_2. For a comparison, electrochemical response of the MoS_2/thionin mixture modified electrode was also recorded. Figure 4 is the CV responses of MoS_2, MoS_2−thionin composite, and MoS_2/thionin mixture. The MoS_2 sheets show nearly no redox peaks. However, the composite displays a pair of redox peaks at $E_{1/2} = -0.22$ V, which is similar to that of the MoS_2/thionin mixture. According to the reported electrochemical behavior of thionin,[30,31] the appearance of these peaks indicates that thionin exists in the composite. But the CV response of the MoS_2−thionin composite is still a little different from the response of the MoS_2/thionin mixture. The redox peaks of the composite are much broader than the peaks of the mixture, and the reduction peak of the composite shifts more negatively than that of the mixture, which means that the MoS_2 sheets donate electrons to thionin to cause the interaction between thionin and MoS_2 sheets. This phenomenon is similar to the electrochemical response of ferrocene-filled carbon nanotubes.[39] Besides, the electrochemical response of the composite is quite stable. Only a slight decrease in current could be observed for the composite after continuous scanning for 50 cycles (Figure 5). Whereas, the peak currents of the MoS_2/thionin mixture decrease quickly after continuous scanning, which implies that

dx.doi.org/10.1021/ac5027786 | Anal. Chem. XXXX, XXX, XXX−XXX

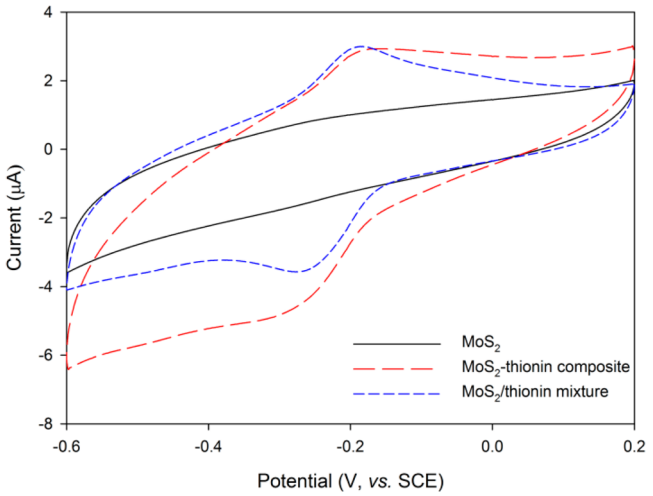

Figure 4. CV responses of the MoS_2, MoS_2–thionin composite and MoS_2/thionin mixture modified electrodes in the N_2 saturated 0.1 M PBS at a scan rate of 50 mV s^{-1}.

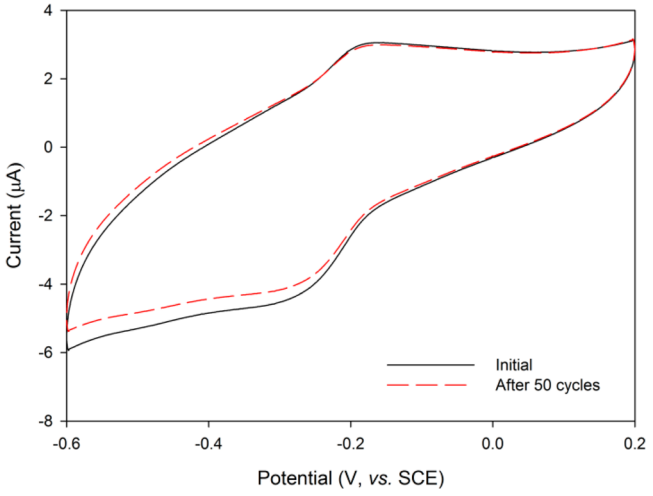

Figure 5. Stability test for the MoS_2–thionin composite modified electrode in the N_2 saturated 0.1 M PBS at a scan rate of 50 mV s^{-1}.

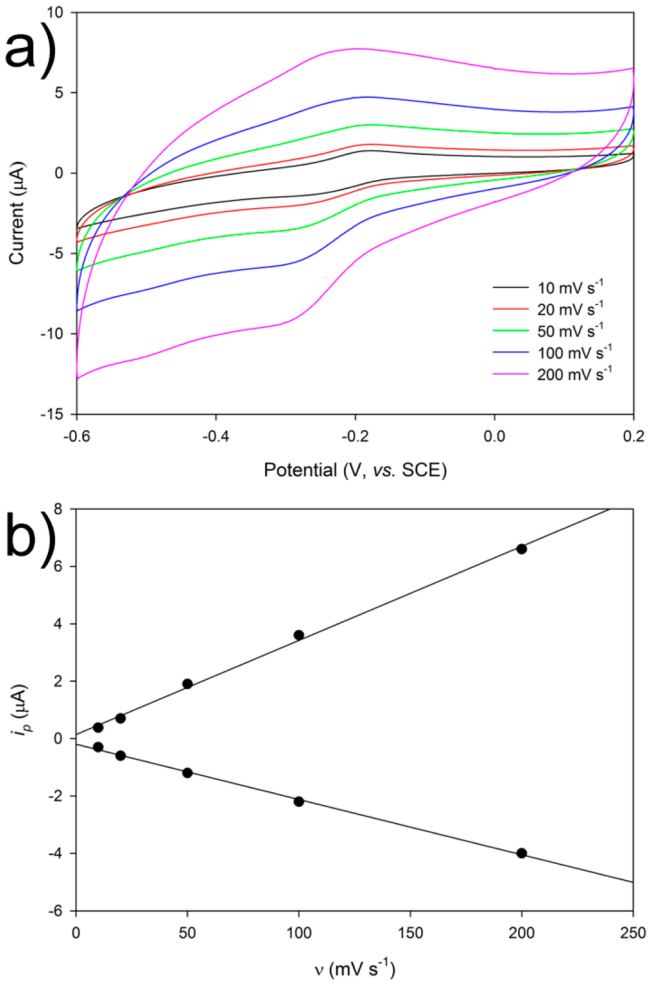

Figure 6. (a) CV responses of MoS_2–thionin composite in the N_2 saturated 0.1 M PBS at different scan rates of 10, 20, 50 , 100, and 200 mV s^{-1}. (b) Plots of the anodic and cathodic peak currents versus the scan rate.

thionin dissociates from the mixture during the scan (Figure S-7). All of these further illustrate that thionin is bound on the MoS_2 sheets during the long-time sonication of MoS_2 and thionin mixture. Moreover, the redox peak currents of the composite increase linearly with the increase of the scan rate from 10 mV s^{-1} to 200 mV s^{-1} (Figure 6), which indicates the characteristic of a surface-confined wave.

The MoS_2–thionin composite modified electrode was then used to determine the concentration of the natural dsDNA based on the interaction of thionin and DNA.[32,40] SWV was chosen to record the current response of the electrode because it is much more sensitive than CV. Figure 7a is the SWV responses of the MoS_2–thionin composite modified electrode in the N_2 saturated 0.1 M PBS without and with the successive injections of dsDNA. In the absence of DNA, one peak appears at −0.27 V vs SCE, which is attributed to the redox of thionin, the other peak at −0.43 V versus SCE corresponds to the redox of the MoS_2 surface defects because the MoS_2 sheets modified electrode displays similar redox current at this potential (Figure S-8). The peak current of the modified electrode at −0.27 V decreases with the increase of dsDNA concentration from 0.09 ng mL^{-1} to even hundreds of ng mL^{-1} due to intercalation and electrostatic interaction of thionin with dsDNA. A linear range over the concentration of dsDNA from 0.09 ng mL^{-1} to 1.9 ng mL^{-1} with a sensitivity of 0.21 μA mL ng^{-1} was obtained (Figure 7b). If the concentration of the detected dsDNA is higher than 1.9 ng mL^{-1}, the sensitivity of the sensor would decrease, even though it could still show response toward the addition of dsDNA. Compared to our previous work based on $Mo_6S_{9-x}I_x$ nanowires,[32] the linear range of this MoS_2-based sensor decreases an order of magnitude for dsDNA detection, which means the sensor in this work has higher sensitivity. The possible reason for this is that MoS_2 sheets provide good sensing platform for immobilization of thionin and interaction of dsDNA with thionin due to plenty of S edges on MoS_2 sheets. The reproducibility of this dsDNA sensor is acceptable. Its relative standard deviation (RSD) is 7.2% for five replicate preparations and measurements at the concentration of 0.94 ng mL^{-1}. What is more, the responses of this sensor are nearly the same for five successive measurements (Figure S-9), which indicates that this sensor could be effective for the sensitive and accurate detection of dsDNA. However, its long-term stability is inferior. After it is incubated in 0.1 M PBS for 24 h, its response currents decrease and its redox potentials shift (Figure S-10) due to the swelling of the modified film, resulting in falling off partially from the electrode surface.

dx.doi.org/10.1021/ac5027786 | Anal. Chem. XXXX, XXX, XXX−XXX

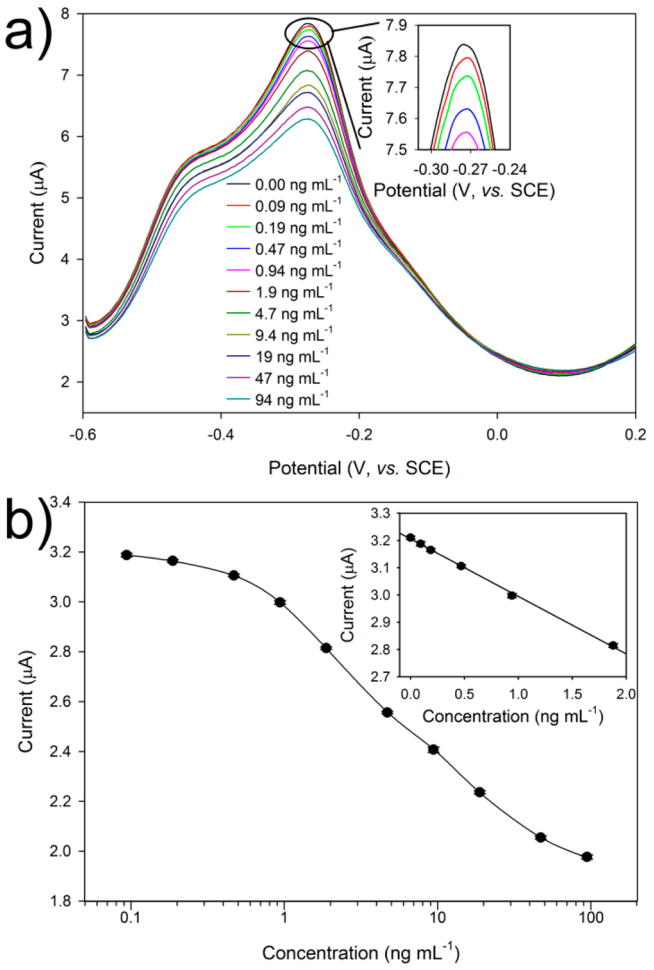

Figure 7. (a) SWV responses of MoS_2−thionin composite modified electrode in the N_2 saturated 0.1 M PBS with the successive injections of dsDNA. (b) The peak current response of the modified electrode to the concentration of the dsDNA. The inset shows the linear part of the curve.

In order to verify the practical use of this dsDNA sensor, the anti-interference effect of the sensor toward protein was also investigated. Figure S-11 shows the SWV response of the sensor with and without 1 μg mL^{-1} bovine serum albumin (BSA). A small decrease in the peak current could be observed with the addition of BSA, and the possible reason is that BSA can adsorb on the modified electrode due to the electrostatic interaction between negatively charged BSA and positively charged thionin, hindering redox of thionin. Because the interference of BSA is not significant, the response of the sensor toward dsDNA in the presence of relatively high concentration of BSA is also characterized. The results prove that this sensor also shows good response with the addition of dsDNA at different concentration levels of ng mL^{-1} to sub ng mL^{-1} even in the presence of 1 μg mL^{-1} BSA (Figure S-12). A linear relationship between the peak current and the concentration of dsDNA from 0.09 ng mL^{-1} to 1.9 ng mL^{-1} is also obtained (Figure S-13). The sensitivity is 0.19 μA mL ng^{-1}, which changes a little compared with that of the sensor in the absence of BSA in the solution. This reveals that the sensor is suitable for the detection of dsDNA in the presence of high concentration of BSA.

In addition to dsDNA, the MoS_2−thionin composite modified electrode also shows response toward ssDNA and RNA because both ssDNA and RNA can be dyed by thionin. This sensor demonstrates a linear response from 0.20 ng mL^{-1} to 2.0 ng mL^{-1} with a sensitivity of 0.17 μA mL ng^{-1} for denatured dsDNA (Figures S-14, S-15) and a sensitivity of 0.14 μA mL ng^{-1} for ssDNA obtained from Aldrich (Figures S-16, S-17), which is similar to those of dsDNA, but for RNA, its sensitivity is lower and its determination limit is higher. A linear response range over RNA concentration from 10 ng mL^{-1} to 200 ng mL^{-1} with a sensitivity of 0.0022 μA mL ng^{-1} was obtained with this sensor (Figures S-18, S-19). It seems that the modified electrode is more sensitive to DNA than RNA. These reveal that the interaction between thionin and polynucleotides involves intercalation and electrostatic interaction. The electrochemical responses of this sensor toward these different kinds of polynucleotides are helpful to expand its application in the field of bioanalysis.

In order to test the suitability of the constructed sensor based on thionin functionalized layered MoS_2 for detection of natural DNA, the sensor was further used to detect the concentration of circulating DNA in human serum. The circulating DNA was extracted from the healthy human serum and then added to the N_2 saturated 0.1 M PBS. A decrease in current could be observed with the addition of DNA extracts (Figure 8). The concentration

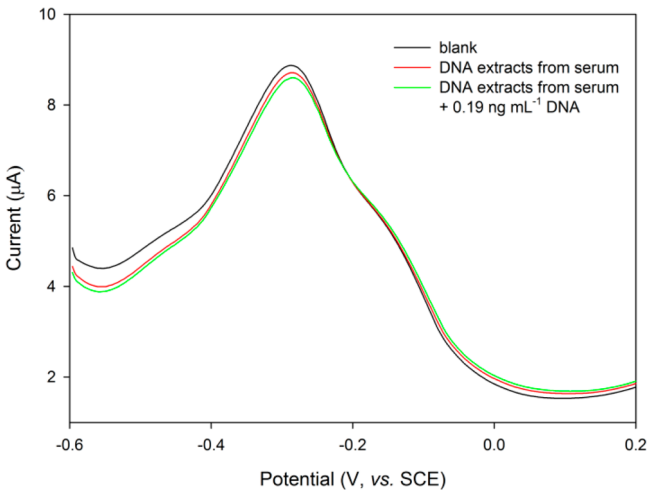

Figure 8. SWV responses of the MoS_2−thionin composite modified electrode in the N_2 saturated 0.1 M PBS with the injection of dsDNA standard sample and DNA extracts from the healthy human serum.

of the circulating DNA in the serum was calculated to be 1.0 ng mL^{-1}, which matched well with the theoretical value of healthy human serum.[19] The recoveries of this biosensor were tested to be 65% ∼ 89% by adding 0.19−0.47 ng mL^{-1} dsDNA into the serum sample solution, which suggested that the result was acceptable. These reveal that this constructed sensor is applicable to the detection of the natural DNA in the real samples.

CONCLUSION

In conclusion, we put forward an extremely easy way to synthesize and modify MoS_2 sheets with the help of ionic liquid 1-butyl-3-methylimidazolium hexafluorophosphate. By sonicating the mixture of MoS_2 and thionin in the ionic liquid, the MoS_2 sheets could be exfoliated from bulk MoS_2 and their surface could be further modified by thionin based on charge transfer. The synthesized MoS_2−thionin composite has been used for construction of a biosensor because it displays stable electrochemical response. The biosensor has been applied to the detection of dsDNA through intercalation and electrostatic interaction of thionin with DNA, resulting in decrease of

dx.doi.org/10.1021/ac5027786 | Anal. Chem. XXXX, XXX, XXX−XXX

electrochemical response, and a linear range over dsDNA concentration from 0.09 ng mL^{-1} to 1.9 ng mL^{-1} could be obtained even in the presence of relatively high concentration of protein. Besides, the biosensor could further be used to detect ssDNA and RNA. The biosensor has been applied to the determination of the extracted circulating DNA from healthy human serum with acceptable results. These suggest that the sensor has promising application potential in bioanalysis and clinical research. Research efforts along these directions are expected to expand the application of MoS_2 greatly in the biosensing field and other fields because this work provides an easy one-step way to obtain functionalized MoS_2 sheets by surface modification. Other molecules containing a thiol group or electron-accepting molecules with structures similar to thionin may also be modified on MoS_2 sheets by this simple method.

■ ASSOCIATED CONTENT

Supporting Information

Supplemental data and figures, including TEM/SEM images, XPS analysis, stability tests, and calibration curves. This material is available free of charge via the Internet at http://pubs.acs.org.

■ AUTHOR INFORMATION

Corresponding Author

*E-mail: lmwx@pku.edu.cn. Tel.: +86 10 62757953. Fax: +86 10 62751708.

Notes

The authors declare no competing financial interest.

■ ACKNOWLEDGMENTS

This work was financially supported by the National Natural Science Foundation of China (Grants 21475003 and 21275010).

■ REFERENCES

(1) Teles, F. R. R.; Fonseca, L. R. *Talanta* **2008**, *77*, 606−623.
(2) Ho, H. A.; Najari, A.; Leclerc, M. *Acc. Chem. Res.* **2008**, *41*, 168−178.
(3) Wang, J. *Anal. Chim. Acta* **2003**, *500*, 247−257.
(4) He, S. J.; Song, B.; Li, D.; Zhu, C. F.; Qi, W. P.; Wen, Y. Q.; Wang, L. H.; Song, S. P.; Fang, H. P.; Fan, C. H. *Adv. Funct. Mater.* **2010**, *20*, 453−459.
(5) Dolatabadi, J. E. N.; Mashinchian, O.; Ayoubi, B.; Jamali, A. A.; Mobed, A.; Losic, D.; Omidi, Y.; de la Guardia, M. *TrAC, Trends Anal. Chem.* **2011**, *30*, 459−472.
(6) Paleček, E.; Bartošík, M. *Chem. Rev.* **2012**, *112*, 3427−3481.
(7) Drummond, T. G.; Hill, M. G.; Barton, J. K. *Nat. Biotechnol.* **2003**, *21*, 1192−1199.
(8) Zhang, X. Z.; Jiao, K.; Liu, S. F.; Hu, Y. W. *Anal. Chem.* **2009**, *81*, 6006−6012.
(9) Jelen, F.; Yosypchuk, B.; Kourilová, A.; Novotný, L.; Paleček, E. *Anal. Chem.* **2002**, *74*, 4788−4793.
(10) Wang, J.; Liu, G. D.; Jan, M. R. *J. Am. Chem. Soc.* **2004**, *126*, 3010−3011.
(11) Wang, J. *Electroanalysis* **2005**, *17*, 7−14.
(12) Zhou, M.; Zhai, Y. M.; Dong, S. J. *Anal. Chem.* **2009**, *81*, 5603−5613.
(13) Wang, Q. B.; Lei, J. P.; Deng, S. Y.; Zhang, L.; Ju, H. X. *Chem. Commun.* **2013**, *49*, 916−918.
(14) Guo, S. J.; Dong, S. J. *TrAC, Trends Anal. Chem.* **2009**, *28*, 96−109.
(15) Wang, J.; Xu, D. K.; Kawde, A. N.; Polsky, R. *Anal. Chem.* **2001**, *73*, 5576−5581.
(16) Sassolas, A.; Leca-Bouvier, B. D.; Blum, L. J. *Chem. Rev.* **2008**, *108*, 109−139.
(17) Wang, J. *Anal. Chim. Acta* **2002**, *469*, 63−71.
(18) Ghosh, I.; Stains, C. I.; Ooi, A. T.; Segal, D. J. *Mol. Biosyst.* **2006**, *2*, 551−560.
(19) García-Olmo, D.; García-Olmo, D. C.; Ontañón, J.; Martinez, E. *Blood* **2000**, *95*, 724−725.
(20) García-Olmo, D. C.; Domínguez, C.; García-Arranz, M.; Anker, P.; Stroun, M.; García-Verdugo, J. M.; García-Olmo, D. *Cancer Res.* **2010**, *70*, 560−567.
(21) Radisavljevic, B.; Radenovic, A.; Brivio, J.; Giacometti, V.; Kis, A. *Nat. Nanotechnol.* **2011**, *6*, 147−150.
(22) Feng, J.; Qian, X. F.; Huang, C. W.; Li, J. *Nat. Photonics* **2012**, *6*, 865−871.
(23) Hinnemann, B.; Moses, P. G.; Bonde, J.; Jørgensen, K. P.; Nielsen, J. H.; Horch, S.; Chorkendorff, I.; Nørskov, J. K. *J. Am. Chem. Soc.* **2005**, *127*, 5308−5309.
(24) Laursen, A. B.; Kegnæs, S.; Dahl, S.; Chorkendorff, I. *Energy Environ. Sci.* **2012**, *5*, 5577−5591.
(25) Wang, T.; Gao, D.; Zhuo, J.; Zhu, Z.; Papakonstantinou, P.; Li, Y.; Li, M. *Chem.—Eur. J.* **2013**, *19*, 11939−11948.
(26) Wang, T.; Zhuo, J.; Chen, Y.; Du, K.; Papakonstantinou, P.; Zhu, Z.; Shao, Y.; Li, M. *ChemCatChem* **2014**, *6*, 1877−1881.
(27) Wang, T. Y.; Zhu, H. C.; Zhuo, J. Q.; Zhu, Z. W.; Papakonstantinou, P.; Lubarsky, G.; Lin, J.; Li, M. X. *Anal. Chem.* **2013**, *85*, 10289−10295.
(28) Song, H. Y.; Ni, Y. N.; Kokot, S. *Biosens. Bioelectron.* **2014**, *56*, 137−143.
(29) Wu, S. X.; Zeng, Z. Y.; He, Q. Y.; Wang, Z. J.; Wang, S. J.; Du, Y. P.; Yin, Z. Y.; Sun, X. P.; Chen, W.; Zhang, H. *Small* **2012**, *8*, 2264−2270.
(30) Zheng, T. T.; Zhang, Q. F.; Feng, S.; Zhu, J. J.; Wang, Q.; Wang, H. *J. Am. Chem. Soc.* **2014**, *136*, 2288−2291.
(31) Wang, Z.; Li, M.; Su, P.; Zhang, Y.; Shen, Y.; Han, D.; Ivaska, A.; Niu, L. *Electrochem. Commun.* **2008**, *10*, 306−310.
(32) Lin, H.; Cheng, H. M.; Liu, L.; Zhu, Z. W.; Shao, Y. H.; Papakonstantinou, P.; Mihailovic, D.; Li, M. X. *Biosens. Bioelectron.* **2011**, *26*, 1866−1870.
(33) Gong, M. J.; Han, T.; Cai, C. X.; Lu, T. H.; Du, J. Y. *J. Electroanal. Chem.* **2008**, *623*, 8−14.
(34) Paleček, E.; Vetterl, V. *Biopolymers* **1968**, *6*, 917−928.
(35) Coleman, J. N.; Lotya, M.; O'Neill, A.; Bergin, S. D.; King, P. J.; Khan, U.; Young, K.; Gaucher, A.; De, S.; Smith, R. J.; Shvets, I. V.; Arora, S. K.; Stanton, G.; Kim, H. Y.; Lee, K.; Kim, G. T.; Duesberg, G. S.; Hallam, T.; Boland, J. J.; Wang, J. J.; Donegan, J. F.; Grunlan, J. C.; Moriarty, G.; Shmeliov, A.; Nicholls, R. J.; Perkins, J. M.; Grieveson, E. M.; Theuwissen, K.; McComb, D. W.; Nellist, P. D.; Nicolosi, V. *Science* **2011**, *331*, 568−571.
(36) Wang, Q. H.; Kalantar-Zadeh, K.; Kis, A.; Coleman, J. N.; Strano, M. S. *Nat. Nanotechnol.* **2012**, *7*, 699−712.
(37) Wang, T. Y.; Liu, L.; Zhu, Z. W.; Papakonstantinou, P.; Hu, J. B.; Liu, H. Y.; Li, M. X. *Energy Environ. Sci.* **2013**, *6*, 625−633.
(38) Chou, S. S.; De, M.; Kim, J.; Byun, S.; Dykstra, C.; Yu, J.; Huang, J. X.; Dravid, V. P. *J. Am. Chem. Soc.* **2013**, *135*, 4584−4587.
(39) Sun, N. J.; Guan, L. H.; Shi, Z. J.; Li, N. Q.; Gu, Z. N.; Zhu, Z. W.; Li, M. X.; Shao, Y. H. *Anal. Chem.* **2006**, *78*, 6050−6057.
(40) Hecht, C.; Friedrich, J.; Chang, T. C. *J. Phys. Chem. B* **2004**, *108*, 10241−10244.